Inorganic Chemistry

ARTICLE

pubs.acs.org/IC

Flexible Diphosphine Ligands with Overall Charges of 0, +1, and +2: Critical Role of the Electrostatics in Favoring Trans over Cis Coordination

Yves Canac,*[,†,‡] Nathalie Debono,[†,‡] Christine Lepetit,[†,‡] Carine Duhayon,[†,‡] and Remi Chauvin*[,†,‡]

[†]CNRS, LCC (Laboratoire de Chimie de Coordination), 205 route de Narbonne, F-31077 Toulouse, France

[‡]Université de Toulouse, UPS, INP, LCC, F-31077 Toulouse, France

Supporting Information

ABSTRACT:

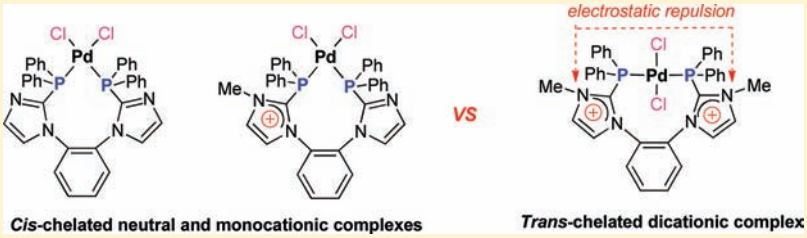

The influence of the formal electrostatic interaction on the cis/trans coordination mode at a $PdCl_2$ center is investigated in a family of isostructural flexible diphosphine ligands $Ph_2P-X-C_6H_4-Y-PPh_2$, where X and Y stand for neutral or cationic N,C-imidazolylene linkers. While the neutral and monocationic diphosphine spontaneously behave as classical cis-chelating ligands, only the dicationic diphosphine, where the electrostatic repulsion between the formal positive charges specifically takes place, is observed to behave as a trans-chelating ligand. The crucial role of electrostatics is analyzed on the basis of ^{31}P NMR data in solution and X-ray diffraction data in the crystal state. Comparative theoretical studies of the cis- and trans-chelated complexes, including EDA, static ^{31}P NMR, MESP, and AIM analyses, have been undertaken on the basis of DFT calculations in the gas phase or in the acetonitrile continuum. Whereas the cis-coordination mode is shown to be thermodynamically favored for the neutral ligand, the trans-coordination mode is found to be preferred for the dicationic homologue. The stereochemical preference is thus shown to be parallel to the expected effect of the formal electrostatic interaction. The results open perspectives for control of the cis- and trans-chelating behavior of flexible bidentate ligands by more or less reversible charge transfer at the periphery of the coordination sphere of a metallic center.

1. INTRODUCTION

The backbone of bidentate L∼L′ ligands plays a fundamental role in the determination of specific properties of their transition metal complexes, in particular in catalysis and asymmetric catalysis. This has been widely illustrated in the design of spectator chelating diphosphine ligands (L, L′ = P) of organometallic catalysts.[1] The length and flexibility of the L∼L′ bridge influence first the ability of the ligand to achieve *chelating* or *bridging* coordination modes. With sufficiently long bridges in appropriate stoichiometry and dilution conditions, the mononuclear chelate mode is favored, at least statistically and kinetically. In the case of complexes with square-planar, bipyramid-trigonal, or octahedral configuration, the same characteristics of the L∼L′ bridge also influence the cis- vs trans-chelating mode preference. Whereas most of the chelate ligands described in the literature have been exclusively, and often implicitly, considered in their preferred cis-coordination mode, the question of the cis- vs trans-coordination preference has been explicitly addressed by the definition of the P−M−P bite angle.[2] In the C_2-symmetric diphosphine series, three classes of chelate ligands are thus distinguished: the strictly cis-chelating ligands (P−M−P ≤ 100°), the intermediate wide-bite-angle ligands (100° < P−M−P ≤ 160°), and the trans-chelating ligands (P−M−P > 160°).[2] Trans-chelating ligands have been particularly exemplified by the TRANSphos,[3] BISBI,[4] and TRAP[5] ligands for their applications in catalysis and asymmetric catalysis (Scheme 1).[6] Purely bidentate trans-chelating diphosphines (without an auxiliary coordinating atom that could drive enforced trans coordination of external P atoms, a situation found in the tridentate pincer complexes) are today attracting a renewed interest.[7] Assuming a sequential coordination process, after coordination of a first P atom, cis or trans coordination of the second P atom is a priori enabled by two degrees of freedom: (i) orientation of the P lone pair by rotation about the bridge−P bond and (ii) adaptation of the metallacycle conformation by rotation about single bonds of the bridge. The bridge may also be

Received: June 24, 2011
Published: October 07, 2011

Scheme 1. Selected Trans-Chelating Ligands with a C_2-Symmetric Core Either Quasi-Exclusive (Rigid Trans-Spanning Ligands, Left)[10] or Adaptative (with Two Internal Degrees of Freedom of the Bridge Indicated by Curved Arrows, Right)

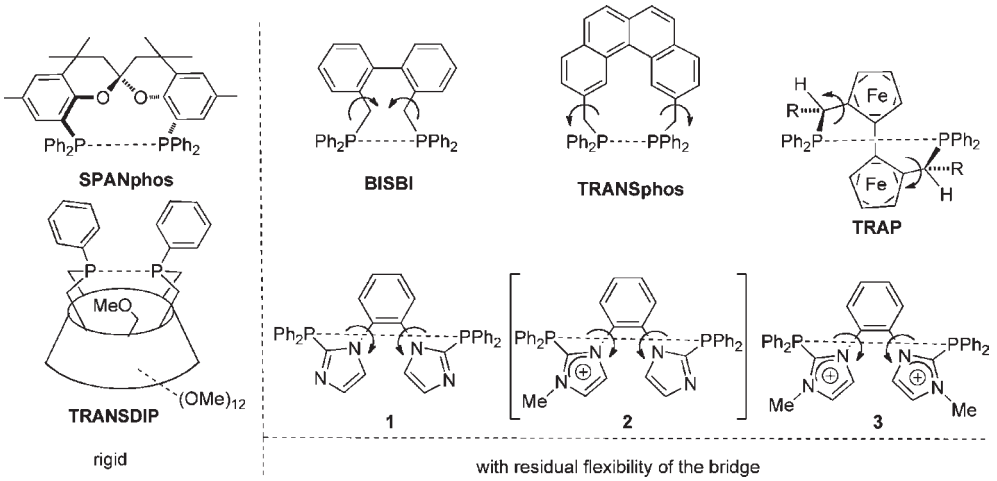

more rigid like in the SPANphos[8] and TRANSDIP[9] ligands, which mainly adopt the trans-coordination mode (trans-spanning ligands: Scheme 1).[10] In most cases, however, residual flexibility of the ligand makes the alternative cis-coordination mode more accessible. If kinetically allowed, the trans−cis isomerization might then proceed either directly (without any P−M bond breaking through a tetrahedral intermediate) or via decoordination of one of the P atoms and possibly through a reservoir of bimetallic species where two L∼L moieties act as bridging ligands between two metallic centers. Nevertheless, known ligands with marked cis- or trans-coordination preference possess backbones with quite different steric demand. Control of the cis- vs trans-coordination mode by minimal alteration of the ligand backbone remains desirable. A controlled switch of the configuration (e.g., by reversible proton, electron, or photon transfer) is an ultimate challenge.

The bis(imidazolylphosphine) **1** based on the *o*-phenylene bridge (Scheme 1) possesses the required characteristics of a trans-chelating ligand while a priori preserving the possibility of acting in a cis-chelating manner through optimized rotation about the Ar−N single bonds. This neutral ligand is sterically very similar (quasi-isosteric) to its N-methylated cationic homologue **2** and its N,N′-dimethylated dicationic derivative **3**. It has been shown that the dication **3** indeed behaves as a versatile cis- or trans-coordinating ligand depending on the environment (especially the formal charge) of a given type of metallic center (Rh(I)): trans-chelating at a neutral RhCl(CO) center (P−Rh−P = 163.8°), cis-chelating at a cationic $[Rh(MeCN)_2]^+$ center (P−Rh^+−P = 96.8°).[11] This configurational change was interpreted by a subtle interplay between electrostatic and orbital effects. After having investigated the change of charge at the metal atom for the given ligand **3**, the change of charge at the ligand backbone for a given neutral metallic center is anticipated to bring out the electrostatic effect only: this is hereafter investigated through the series of homologous quasi-isosteric ligands **1**−**3** at the neutral homoleptic $PdCl_2$ center.

Structural effects of the attractive interaction between formal point charges of opposite signs in the coordination sphere of transition metals have been explicitly addressed on examples of either metal−ligand[12] or ligand−ligand electrostatic interactions.[13] Likewise, the repulsive interaction between two negative (SO_3^-, PO_3^{2-}) or two positive (R_4N^+, R_4P^+) formal charges has also been reported to dictate the trans preference of pairs of anionic or cationic monophosphines, respectively.[14] In the latter cases, however, the electrostatic effect is assisted by the steric effect, also repulsive in nature and thus favoring trans arrangements. Even if steric and electrostatic effects remain globally stronger than the antisymbiotic electronic effect (HSAB cis preference or trans influence for class b soft metallic centers),[15] the contribution of the electrostatic component is generally quite weak as the interacting formal charges are located at the periphery of the ligand and thus remote from the metallic center. In the ligand **3** the charges are located as closely as possible to the metal center and even formally at the coordinating P atoms themselves: since imidazoliophosphines have been demonstrated to be true NHC-phosphenium adducts,[16] the formal positive charge can be considered to be more concentrated at the P atoms than at the adjacent C and N atoms (at least as soon as the semipolar form N_2C^+−P of the dative N_2C−>P^+ bond is not invoked).

Moreover, the bidentate and flexible nature of **3** is anticipated to lower the purely steric effect on the trans to cis preference ratio. If the quasi-isosteric ligands **1** and **2** (where formal electrostatic repulsion is absent) exhibited a cis-chelating behavior, a second example of the trans-chelating behavior of **3** (at a $PdCl_2$ center instead of a Rh(CO)Cl center) would provide further support to an interpretation based on electrostatic effects in the corresponding complexes.[11]

2. RESULTS AND DISCUSSION

2.1. Experimental Results. Following a recently described procedure (Scheme 2),[11] the neutral and dicationic diphosphines **1** and **3** were prepared from the readily available 1,2-bis(imidazol-*N*-yl)benzene and characterized by X-ray diffraction analysis of corresponding single crystals (Figure 1 and Table 1).[17] Addition of a single equivalent of MeOTf to the neutral diphosphine **1** in CH_2Cl_2 afforded the monocationic diphosphine **2** in 70% yield (Scheme 2). The ionic nature of **2** is indicated by its low solubility in nonpolar solvents, and its dissymmetric structure is confirmed by two coupled inequivalent ^{31}P NMR signals at δ = −22.9 (d, N_2C^+P) and −31.8 (d, N_2CP) ppm (J_{PP} = 28.3 Hz) and by

dx.doi.org/10.1021/ic201342z |*Inorg. Chem.* 2011, 50, 10810–10819

Scheme 2. Selective N-Methylation of the Neutral Diphosphine 1 to the Mono- and Dicationic Diphosphines 2 and 3

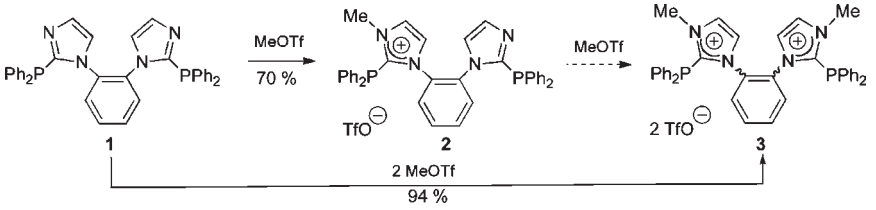

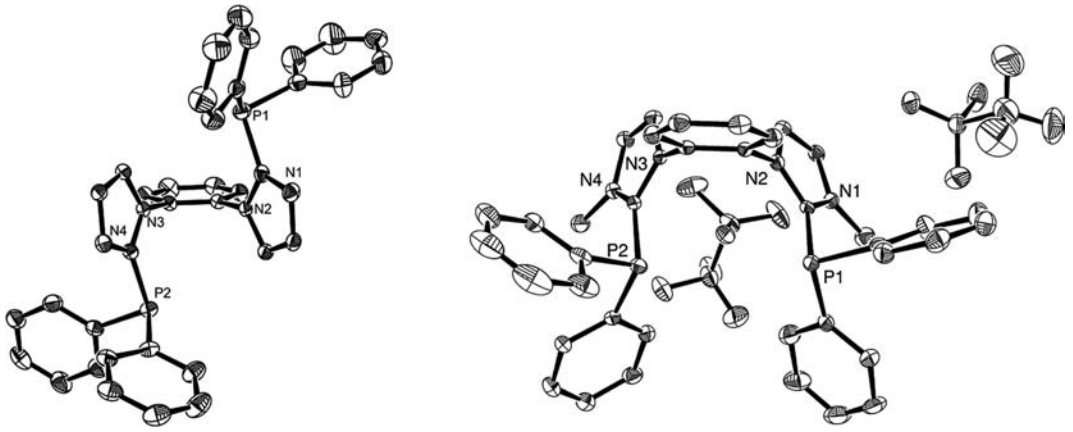

Figure 1. ORTEP views of the X-ray crystal structures of ligands **1** (left) and **3** (right) (Scheme 2) with thermal ellipsoids drawn at the 30% probability level (for clarity, H atoms were omitted). See Table 1 for details.

Table 1. Selected Bond Lengths [Å] and Angles [deg] from X-ray Diffraction Analyses of Ligands 1 and 3 and Their Respective Complexes 4, 5, and 6

	1[a]	3[b]	4	5	6
C_1-P_1	1.820(2)	1.845(4)	1.809(4)	1.836(4)	1.839(4)
$C_{10}-P_2$	1.824(2)	1.831(5)	1.801(4)	1.818(5)	1.836(3)
C_1-N_1	1.317(3)	1.358(6)	1.306(5)	1.356(6)	1.338(4)
C_1-N_2	1.371(3)	1.347(6)	1.371(5)	1.356(6)	1.361(4)
$C_{10}-N_3$	1.371(3)	1.362(6)	1.373(5)	1.381(6)	1.347(4)
$C_{10}-N_4$	1.317(3)	1.314(6)	1.312(5)	1.322(6)	1.338(4)
P_1-Pd			2.2349(9)	2.2973(11)	2.2880(9)
P_2-Pd			2.2676(9)	2.2983(12)	2.2918(9)
$Pd-Cl_1$			2.3475(10)	2.3306(13)	2.3138(9)
$Pd-Cl_2$			2.3194(9)	2.3245(11)	2.2723(9)
P_1-Pd-P_2			93.22(3)	97.17(4)	165.72(3)
$Cl_1-Pd-Cl_2$			91.69(4)	88.47(4)	178.38(4)

[a] The neutral molecule **1** is quasi-C_2 symmetric with the two neutral imidazolylphosphine moieties in the anti position with respect to the 1,2-phenylene bridge. [b] The dication **3** is quasi-C_s symmetric with the two imidazoliophosphine moieties maintained in the syn position with respect to the 1,2-phenylene bridge by an intercalated triflate anion (electrostatic pincer, see Scheme 4). In MeCN solution, **3** appears as a mixture of two atropisomers, possibly corresponding to the quasi-C_2 and quasi-C_s conformers.

the 3-*H* integral of the $N-CH_3$ ^{1}H NMR signal at δ = +3.22 ppm.

Treatment of the diphosphines **1**, **2**, and **3** with a stoichiometric amount of $(PhCN)_2PdCl_2$ in THF at room temperature

Scheme 3. Preparation of $PdCl_2$ Complexes 4−6 of the Neutral and Cationic Diphosphines 1−3

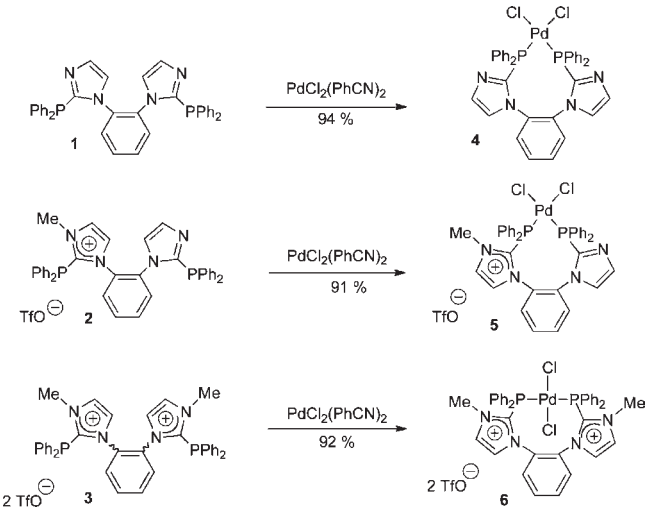

afforded the corresponding $PdCl_2$ complexes **4**, **5**, and **6** in 94%, 91%, and 92% yield, respectively (Scheme 3).[18] The $^{31}P\{^1H\}$ NMR spectrum of **4** and **6** displays a singlet at 8.8 and 9.2 ppm, respectively, while that of the dissymmetric complex **5** exhibits two singlets at 4.1 and 10.6 ppm, in the typical range for Pd−diphosphine complexes.[19] The absence or very weak value of the J_{PP} coupling constant is indicative of a cis arrangement of ligand **2** in **5** (see calculated spectra, section 2.2.2). All complexes were thus formed as single isomers at the NMR time scales at room

dx.doi.org/10.1021/ic201342z |*Inorg. Chem.* 2011, 50, 10810–10819

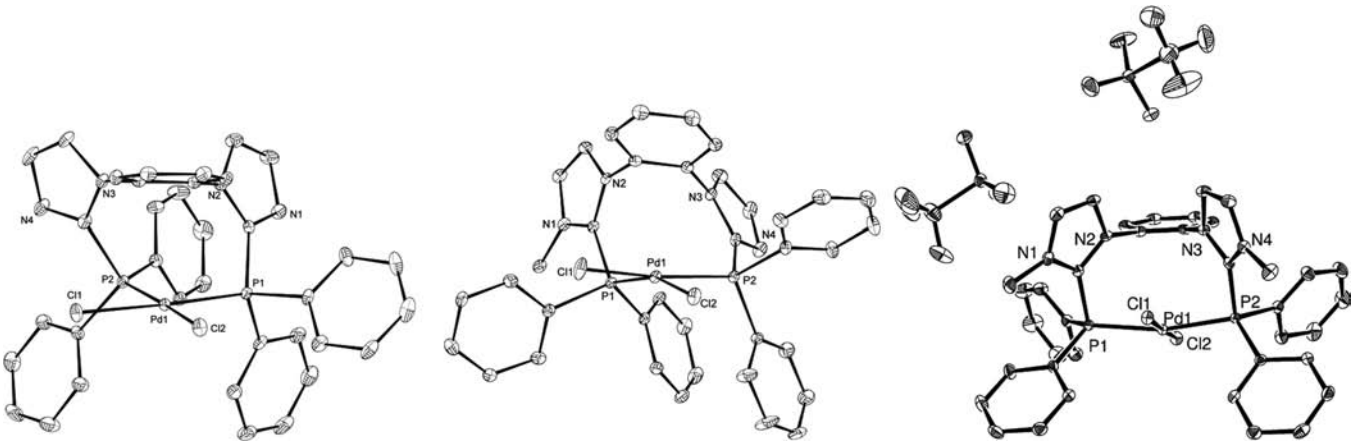

Figure 2. ORTEP views of the X-ray crystal structures of the palladium complexes **4** (left), **5** (middle), and **6** (right) (Scheme 3) with thermal ellipsoids drawn at the 30% probability level (for clarity, triflate anions and H atoms were omitted, except for **6**). See Table 1 for details.

Scheme 4. Representation of the Pincer $PC^{+}\cdots O^{-}\cdots {}^{+}CP$ Attractive Electrostatic Interaction Inducing the Syn Conformation of 3 in the Crystal State (See Figure 3)

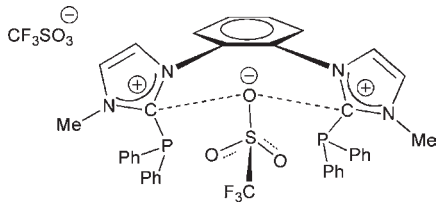

temperature. The ^{31}P and ^{1}H NMR spectra of the complexes showed neither decoalescence nor peak broadening in CD_3CO-CD_3 at low temperature (down to −50 °C), suggesting that the dynamics of the complexes is limited to low-energy conformational changes without cis/trans interconversion at room temperature.

All complexes, including the *electrostatically strained* dicationic complex **6**, proved to be thermally stable in air both in solution and in the solid state. Their exact structure was determined by X-ray diffraction analysis of single crystals deposited at room temperature from $CHCl_3$ for **4**, CH_2Cl_2 for **5**, and CH_3CN/Et_2O for **6** (Figure 2, Table 1).[17]

Whereas the square-planar-type configuration is almost perfect in complex **4** (five atoms in the quasi-coplanar P_2PdCl_2 motif), it is distorted in both complexes **5** (four atoms in quasi-coplanar $PPdCl_2$ or P_2PdCl motifs, from which the remaining Pd−P or Pd−Cl bond is tilted by ca. 17.6°) and **6** (four atoms of the $PPdCl_2$ motifs, including a quasi-linear $PdCl_2$ unit, from which the second Pd−P bond is tilted by ca. 14.3°). In all complexes, however, the palladium atom occupies a position such that the sum of the four successive bond angles at Pd is close to that of the planar geometry ($\Sigma° = 360 \pm 1.8°$), far from the tetrahedral geometry (for which, ideally, $\Sigma° = 438°$). The P−Pd−P bite angles (and corresponding Cl−Pd−Cl angles) are equal to 93.2° (91.7°), 97.2° (88.5°), and 165.7° (180°) for **4**, **5**, and **6**, respectively. Clearly, the diphosphine ligands act in a cis-chelating manner in **4** and **5** and in a trans-chelating manner in **6**. The trans-chelating behavior at the neutral $PdCl_2$ center is therefore specific of the sole ligand **3**, where electrostatic repulsion between positive formal charges occurs. This result is a second example of the previously reported trans-chelating behavior of **3** at neutral late transition metal centers, namely, $PdCl_2$ and RhCl(CO) centers.[11]

The chelation mode is naturally correlated with the range of distances between the atoms where the positive charges are formally located upon of N-methylation of imidazolyl rings of **4**, namely, the N, C, and P atoms of the facing N_2C−P moieties (MeN_2C:−> $P^{+} \leftrightarrow MeN_2C^{+}-P \leftrightarrow MeN^{+}{=}C(N)-P$). For a first-level comparative purpose, the average location of the formal charge is assumed to be the centroid of these four atoms, namely, the C atom.[16]

The P···P and C···C distances are thus, respectively, close to 3.36 and 3.98 Å (±0.1 Å) in complexes **4** and **5** and are much greater at 4.54 and 4.61 Å in complex **6** (Table 1). The formal electrostatic repulsion occurring in **6** can be reasonably assumed to be the driving force of the change in chelation mode of the flexible ligand by passing from complexes **4** and **5** (without formal electrostatic strain) to complex **6**.

It is however noteworthy that in the crystal state the free ligands **1** and **3** seem to freely adopt conformations where the C···C distances are identical (4.24 ± 0.04 Å) and where the P···P distance is even shorter in free **3** (4.21 Å) than in the chelate complex **6** (4.54 Å) (Table 1). At first sight, this suggests that the zeroth-order analysis of the formal electrostatic repulsion effect might not apply to the free ligands. Nevertheless, inspection of the X-ray crystal structures indicates that the dicationic diphosphine adopts the same conformation in the free state **3** and in the trans-chelated state **6**, where the two imidazoliophosphine moieties reside in the syn position with respect to the 1,2-phenylene bridge (Figures 1 and 2, and Scheme 4). This syn arrangement is imposed by the P−Pd−P chelation in complex **6** and by a $PC^{+}\cdots O^{-}\cdots {}^{+}CP$ electrostatic pincer at a negatively charged oxygen atom of an intercalated triflate anion ($C^{+}\cdots O^{-} = 3.38 \pm 0.06$ Å) in the free ligand **3** (for steric reasons, no triflate anion is intercalated in **6** and the two neutral imidazolylphosphine moieties of the free ligand **1** reside in the anti position with respect to the 1,2-phenylene bridge).

The paradox is therefore explained by an electrostatic attractive interaction between the triflate anion and the two cationic moieties of ligand **3**. The triflate anion thus screens the facing positive charges, compensates for their repulsion, and induces a specific electrostatic packing in the crystal state.

dx.doi.org/10.1021/ic201342z |*Inorg. Chem.* 2011, 50, 10810–10819

Table 2. Relative Energies of the Cis and Trans Isomers of Complexes 4-6 Calculated at Various Levels Using the 6-31G/LANL2DZ*(Pd) Basis Set[a]**

	PBE	B3PW91	M05-2X	COSMO-PBE	PCM-PBE	PCM-B3PW91	ZPE[b]
cis-**4**	0.0	0.0	0.0	0.0	0.0	0.0	0.0
trans-**4**	2.91	0.66	4.22	4.96	6.76	4.81	4.29
cis-**5**		11.39	9.61	0.0	0.0	1.64	2.32
trans-**5**		0.0	0.0	0.77	0.53	0.0	0.0
cis-**6**		19.19	17.81	6.63	4.76	7.35	7.38
trans-**6**		0.0	0.0	0.0	0.0	0.0	0.0

[a] Energies are given in kcal/mol. PCM and COSMO methods were used to take into account the acetonitrile solvent (ε = 35.688). [b] Zero-point-corrected energies from PCM-B3PW91 calculations.

Table 3. Calculated (PCM-B3PW91) and Experimental Data for Selected Geometrical Parameters of Pd Complexes 4−6 (Bond Lengths in Å, Bond Angles in deg)[a]

Pd complex		Pd−P	Pd−Cl	P−CN_2	P−Pd−P	Cl−Pd−Cl
cis-**4**	exp. XRD	2.235	2.319	1.809	93.2	91.7
		2.268	2.348	1.801		
	calcd	2.310	2.392	1.821	94.6	89.3
		2.326	2.410	1.823		
cis-**5**	exp. XRD	2.297	2.331	1.836	97.17	88.47
		2.298	2.325	1.819		
	calcd	2.284	2.339	1.862	98.4	88.5
		2.289	2.322	1.818		
trans-**6**	exp. XRD	2.288	2.314	1.839	165.7	178.4
		2.292	2.272	1.836		
	calcd	2.354	2.333	1.860	164.5	177.5
		2.358	2.387	1.861		

[a] All calculations were performed with the 6-31G**/LANL2DZ*(Pd) basis set.

Though possibly trans chelating, as observed in complex **6**, the dicationic ligand **3** is not trans spanning and might also be able to behave in a cis-chelating manner. Whatever is the origin of the stereochemical preference (electrostatic vs orbital vs steric), one main question is whether the observed trans chelation of the dicationic ligand **3** in **6** results from thermodynamic or kinetic control. This point and others are addressed below by resorting to computational methods.

2.2. Computational Analysis. *2.2.1. Optimized Structures and Energies.* The relative stability of the cis and trans isomers of complex **4** and complex ions **5** and **6** (in the absence of triflate anion) was investigated at various DFT levels (Table 2) either in the gas phase or taking into account the acetonitrile solvent via a continuum dielectric medium as implemented in the PCM or COSMO methods. The *trans*-**4** and *trans*-**6** complexes were calculated to be C_s symmetric, whereas all other complexes were found to exhibit a C_1 symmetry.

In the absence of anion, the same stereochemical stability order is found for the neutral and dicationic complexes **4** and **6** whatever the calculation level: *cis*-**4** is more stable than *trans*-**4**, and *trans*-**6** is more stable than *cis*-**6**. The calculated thermodynamic data are thus in qualitative agreement with the stereochemical preferences observed in the crystal state (see preceding section). The relative energy values of the isomers are sensitive to the calculation level (Table 2), but PCM or COSMO calculations in the acetonitrile continuum are expected to be more reliable. In such a polar solvent, the anion−cation interactions are a priori weakened and the presence of the triflate anions of **6** can indeed be neglected. The latter methods thus suggest an energy difference of ca. 6 ± 1 kcal/mol between the cis and the trans isomers of **4** and **6**. Gas-phase calculations, including M05-2X calculations expected to account for weak intramolecular interactions, deviate strongly from this value.

The calculated structures are in good agreement with the available X-ray crystal data (Tables 1 and 3). As previously reported for calculations using the same LANL2DZ* pseudopotential for the Pd atom, Pd−P and Pd−Cl bonds and to a lesser extent P−C bonds are calculated to be longer (up to 0.1 Å) than in the experimental structures.[20] As M05-2X does not perform better than B3PW91 for both *cis*-**4** and *trans*-**6** (see Supporting Information, Tables S1 and S2), the PCM-B3PW91 level was selected as an optimal compromise for further studies.

The energy calculation results are thus parallel to the experimental observations but do not give any hint about the possible electrostatic origin of the difference in the stereochemical preference of **4** and **5**. Indeed, the steric hindrance provided by the assumed quasi-isosteric ligands **1**−**3** is indeed not strictly equivalent because of the presence or absence of *N*-methyl substituents. In spite of the smallness and peripheral position of the methyl groups, steric effects cannot be ruled out a priori for explaining the trans preference of the dicationic complex **6**. Dispersive interactions between the methyl groups and phenyl substituents of the adjacent PPh_2 fragments might indeed be ultimately responsible for a steric relaxation from *cis*-**6** to *trans*-**6**, but the difference has been checked to be nonsignificant (the shortest distance between carbon atoms of two such fragments is calculated at 3.17 Å in *trans*-**6** vs 3.12 Å in *cis*-**6**).[21]

Between the extreme cases of the neutral and dicationic complexes **4** and **6**, the intermediate case of the monocationic complex **5** deserved particular attention. The calculated structure of *cis*-**5** optimized at PCM-B3PW91 (in acetonitrile) was found to be in good agreement with the X-ray diffraction analysis data (Table 3). The relative energy calculation results for *cis*-**5** and *trans*-**5** are however less conclusive. Indeed, whereas gas-phase calculations are in favor of a cis-coordination mode, PCM and COSMO calculations in acetonitrile solvent suggest that the cis and trans isomers of **5** are almost isoenergetic (Table 2). The *trans*-**5** isomer is predicted to be more stable than *cis*-**5** at the B3PW91 level, while the reverse is predicted at the PBE level, in agreement with the observation in the crystal state. The lower energy difference between the isomers of **5** (as compared to the corresponding isomers of **4**) cannot be explained by a formal electrostatic repulsion: in contrast to **3** and **6**, indeed, a single

formal positive charge occurs in **2** and **5**. This illustrates the fact that electrostatics is just a competing contribution in the general case. Nevertheless, the trans isomer remains much less stabilized in the monocation **5** than in the dication **6**.

The quasi-degeneracy of the *cis*-**5** and *trans*-**5** cations suggests kinetic control in the stereoselective formation of the cis isomer. However, although the scenario of a very fast *cis*-**5** ⇄ *trans*-**5** interconversion at the NMR time scales accompanied with a shift toward the cis isomer upon crystallization could be ruled out on the basis of the general knowledge on Pd(II) complexes,[22] confirmation was required. This point is addressed in the next section by comparing the calculated NMR spectra of *cis*-**5** and *trans*-**5** cations.

2.2.2. Static NMR Spectrum of Complex ***5***. Although variable-temperature NMR analyses of complex **5** did not allow us to reveal any equilibrium between interconverting species, the cis and trans isomers of the cation were calculated to be close in energy (see Table 2). Nevertheless, the vanishing value of the J_{PP} coupling constant strongly suggests the occurrence of the sole cis-coordinated complex (vide supra). In order to confirm this point, the ^{31}P NMR chemical shifts and corresponding J_{PP} coupling constants in the equilibrium structures of *cis*-**5** and *trans*-**5** were calculated at 0 K and compared with results on a series of related Pd complexes described in ref 15a and 17 (Table 4 and Supporting Information, Table S3). In accordance with previously reported NMR data for *trans*-diphosphine Pd complexes, a large value is calculated for *trans*-**5** (J_{PP} = 416.4 Hz) whereas a much lower value is calculated for *cis*-**5** (J_{PP} = −15.6 Hz). The latter value and its difference with the former are therefore in agreement with the occurrence of the *cis*-**5** isomer as the major species in solution, as it could be expected.

2.2.3. Energy Decomposition Analysis (EDA). In spite of the above proposed qualitative arguments on a possible electrostatic origin of the stereochemical inversion observed for complexes **4** and **6**, electrostatics provides only a contribution to the global interaction. From a quantitative viewpoint, EDA allows for partitioning the interaction energy (E_{int}) between two fragments into three components resulting from three types of interactions, namely, (i) the Pauli repulsion (E_{Pauli}), (ii) the electrostatic interactions (E_{elstat}), and (iii) the orbital overlaps (E_{orb}). The latter accounts for the charge transfer induced by the interaction between occupied and empty orbitals not belonging to the same fragment and for polarization effects corresponding to the mixing of orbitals within each fragment.

EDA of the interaction between the neutral $PdCl_2$ fragment and the neutral or cationic ligand **1**, **2**, or **3** frozen in the geometry adopted in the corresponding complex was performed for complexes **4**−**6**. Following the Morokuma−Ziegler scheme implemented in the ADF program package,[23] the EDA results are listed in Table 5. This EDA study allows us to investigate the role of electrostatics in the metal−ligand interaction and provides only indirect insight into the origin of the cis/trans stereochemical preference of ligands **1**−**3**.[24]

In the three complexes, the total interaction energy E_{int} is close to −4.0 kcal/mol, a rather small value as compared to other reported Pd−phosphine complexes.[25] In all cases, the electrostatic term dominates the orbital term in the total *attractive* interaction energy $E_{attr} = E_{orb} + E_{elstat}$, with a E_{elstat}/E_{attr} ratio remaining very close to 60% (Table 5). Although the electrostatic term intervenes for ca. 1/3 in the sum of the three absolute interaction terms of the EDA ouput, it is equal to ca. 2/3 of the sum of the absolute electrostatic and quantum terms (Table 5, columns 9 and 8). These values are thus approximately the same for all complexes and illustrate the importance of the electrostatic interaction in chemical bonding.[26] It is also noteworthy that whatever is the criterion used, the contribution of the electrostatic term is systematically higher for the most stable isomer of each pair of isomers of **4**, **5**, and **6**.

2.2.4. AIM Topological Analysis. Topological analysis of the electron density provides a partition of the molecular space into atomic basins and allows for estimation of the corresponding

Table 4. Calculated ^{31}P Chemical Shifts and J_{PP} Coupling Constants for *cis*-5, *trans*-5, and *trans*-6[a]

	δ^{31}P (ppm)		J_{PP} (Hz)	
	calcd	exp.	calcd	exp.
cis-**5**	**44.6**	10.6	−15.6	0
	19.7	4.1		
trans-**5**	**27.4**	na	416.4	na
	43.9	na		
trans-**6**	**37.5**	9.2	432.5	
	37.5			equiv. P

[a] B3PW91/6-31+G**/LANL2DZ*(Pd) level of calculation.

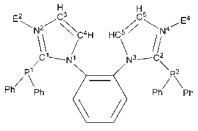

Figure 3. Atom labeling for the AIM analysis of the diphosphine ligands in complexes **4**−**6** (see Table 6). The E^2 and E^4 substituents at the N^2 and N^4 atoms, respectively, denote either lone pairs (LP) or methylium groups (CH_3^+).

Table 5. Energy Decomposition Analysis of Complexes 4−6 (Optimized at the PCM-B3PW91/6-31G/LANL2DZ*(Pd) Level)[a]**

	E_{Pauli}	E_{elstat}	E_{orb}	E_{int}	E_{int}/E_{elstat}	E_{elstat}/E_{attr}[b]	$\lvert E_{elstat}\rvert/[\lvert E_{elstat}\rvert + \lvert E_{quant}\rvert]$[c]	$\lvert E_{elstat}\rvert/(\lvert E_{elstat}\rvert + \lvert E_{Pauli}\rvert + \lvert E_{orb}\rvert)$[d]
trans-**4**	15.448	−11.974	−9.362	−4.889	0.446	0.540	0.643	0.307
cis-**4**	11.030	−9.501	−6.153	−4.625	**0.487**	**0.607**	**0.661**	**0.356**
trans-**5**	10.910	−9.553	−5.984	−4.628	**0.484**	**0.615**	**0.660**	**0.361**
cis-**5**	10.747	−8.858	−5.879	−3.990	0.450	0.601	0.645	0.348
trans-**6**	10.987	−9.417	−5.988	−4.418	**0.469**	**0.611**	**0.653**	**0.357**
cis-**6**	11.414	−9.095	−6.144	−3.824	0.421	0.597	0.633	0.341

[a] Energies are given in kcal/mol. [b] Ratio of the electrostatic interaction term to the total energy of attractive interactions ($E_{attr} = E_{elstat} + E_{orb}$). [c] Ratio of the absolute electrostatic term to the sum of the absolute electrostatic and quantum terms ($E_{quant} = E_{Pauli} + E_{orb}$). [d] Ratio of the absolute electrostatic term to the sum of the three absolute terms of EDA. Values for the most stable isomer are given in bold.

dx.doi.org/10.1021/ic201342z |*Inorg. Chem.* 2011, 50, 10810–10819

Table 6. AIM Atomic Charges of the Cis and Trans Isomers of Complexes 4−6[a]

		Pd	P^1	P^2	C^1	C^2	N^1	N^2	N^3	N^4	CH_3	Cl
4	cis	0.30	1.82	1.79	0.47	0.48	−1.30	−1.20	−1.30	−1.20		−0.54
E^2 = LP	trans	0.32	1.80	1.80	0.49	0.49	−1.30	−1.20	−1.30	−1.20		−0.54
E^4 = LP												
5	cis	0.31	1.74	1.78	0.58	0.47	−1.30	−1.20	−1.30	−1.30	0.26	−0.50
E^2 = LP	trans	0.33	1.73	1.84	0.59	0.49	−1.30	−1.20	−1.30	−1.30	0.26	−0.50
$E^4 = Me^+$												
6	cis	0.31	1.75	1.70	0.58	0.58	−1.30	−1.30	−1.30	−1.30	0.25	−0.50
$E^2 = Me^+$	trans	0.34	1.75	1.75	0.6	0.6	−1.30	−1.30	−1.30	−1.30	0.25	−0.50
$E^4 = Me^+$												

[a] Atom labeling in Figure 3. B3PW91/6-31G**/DGDZVP(Pd)//PCM-B3PW91/6-31G**/LANL2DZ*(Pd) level of calculation.

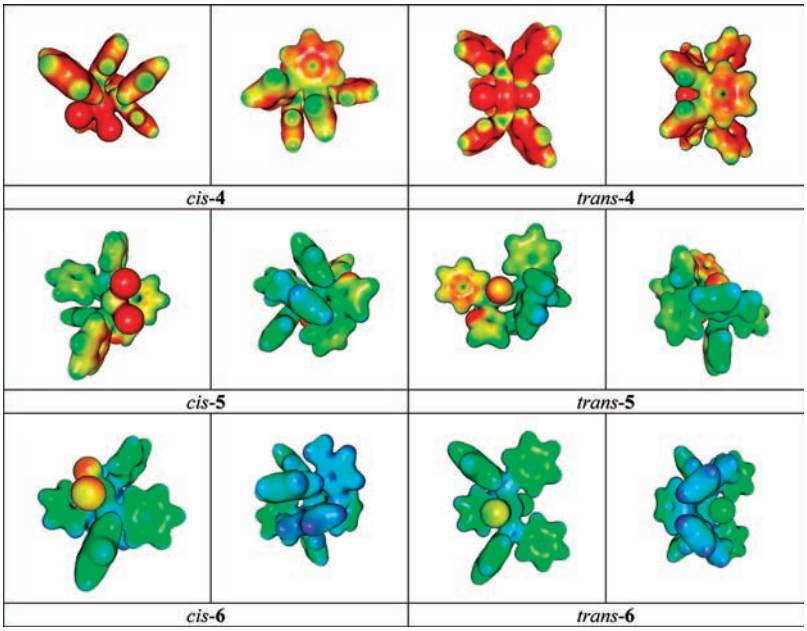

Figure 4. Isodensity surface (0.02 au) color coded with the MESP of complexes **4**−**6** (optimized at the PCM-B3PW91/6-31G**/LANL2DZ*(Pd) level). Color scale: red MESP < 0.05; yellow MESP = 0.1; green MESP = 0.20; light-blue MESP = 0.30; dark-blue MESP > 0.45.

atomic AIM (atoms in molecules) charges.[27] AIM analysis of complexes **4**−**6** was performed using either the available experimental XRD geometry or the calculated structure in the acetonitrile continuum (Figure 3, Table 6).

In each pair of isomers, the AIM charges of all the atoms in the coordination sphere are very similar. The negative AIM charges are located at the N and Cl atoms and do not depend on neither the remote environment (beyond the E^i substituents for the N atoms) nor on the stereochemistry (Table 6). The same trend applies to the positively charged atoms in the whole series: the Pd atoms (q_{Pd} = +0.32 ± 0.02 e), the neutral phosphine P atoms (q_P = +1.81 ± 0.03 e), the phosphenium P atoms (q_P = +1.73 ± 0.02 e), the P-bonded imidazolyl C atoms (q_C = +0.48 ± 0.01 e), and the P-bonded imidazolium C atoms (q_C = +0.59 ± 0.01 e). The C and P atoms of the N_2C-P unit exhibit opposite charge sensitivities upon N-methylation (E^i: LP → Me, ΔQ = +1 e): a natural sensitivity for the C atom ($\Delta q_C \approx$ +0.1 e) and an unnatural one for the P atom ($\Delta q_P \approx -$ 0.08 e). The excess positive charge is spread over the N-methylated imidazole ring, and the increase of positive charge at the C^1 and C^2 atoms is compensated by a decrease of the positive charge at the adjacent P atoms.

2.2.5. Molecular Electrostatic Potential (MESP). The molecular electrostatic potential (MESP) is the potential generated by the molecular charge distribution as experienced by a positive point charge[28]

$$V(r) = \sum_A \frac{Z_A}{|r - R_A|} - \int \frac{\rho(r')}{|r - r'|} d^3r'$$

where Z_A denotes the nuclear charges, R_A the position of the nuclei, and $\rho(r)$ the electron density. The MESP minima indicate the sites of concentration of the electron density and the most favorable sites for electrophilic attack.[29] Exploration of positive MESP regions are visualized by MESP-textured isodensity surfaces, as shown in Figure 4 for complexes **4**−**6**.

Regions of increasing positive MESP are clearly building up by shifting from the neutral complex **4** to the dication **6**, through the intermediate monocation **5**. For the dication **6**, large positive MESP values (dark blue) appear to be more equally distributed

dx.doi.org/10.1021/ic201342z |*Inorg. Chem.* 2011, 50, 10810–10819

in the most stable *trans*-**6** isomer than in the *cis*-**6** isomer. This illustrates that electrostatic repulsion is globally reduced by trans coordination of the dicationic diphosphine **3** by comparison with cis coordination of the same ligand. This also tends to confirm that the driving force of the observed trans-coordination preference of **3** in **6** is at least partly of electrostatic nature.

CONCLUSION

The trans-chelating character of the flexible generic diphosphines **1**−**3** has been shown to be governed by the formal electrostatic interaction, the two positive charges of the dicationic ligand specifically repelling the coordinating P atoms in trans positions at a $PdCl_2$ center. The combined effects of the electron-poor and trans-chelating characters of this dicationic ligand in homogeneous catalysis deserve now to be investigated. From a still more speculative viewpoint, the results start to pave the way to a reversible control of the cis- and trans-chelating behavior of flexible (non-trans-spanning) bidentate ligands by proton transfer (instead of the irreversible methylation process investigated here) outside the coordination sphere of the metal atom.

COMPUTATIONAL DETAILS

Geometries were fully optimized at the B3PW91/6-31G**/LANL2DZ*-(Pd) level of calculation using Gaussian09.[30] LANL2DZ*(Pd) means that f-polarization functions derived by Ehlers et al.[31] for Pd have been added to the LANL2DZ(Pd) basis set. Vibrational analysis was performed at the same level as the geometry optimization. Solvent effects were included using the polarizable continuum model (PCM) implemented in Gaussian09[30] or the conductor-like screening model (COSMO)[32] implemented in ADF 2008.01.

The magnetic shielding tensor and nuclear spin coupling constants were calculated at B3PW91/6-31+G**/LANL2DZ*(Pd) using the GIAO (gauge-independent atomic orbital) method implemented in Gaussian09.[30] The ^{31}P NMR chemical shifts were estimated with respect to the usual H_3PO_4 reference.

The gas-phase molecular electrostatic potential (MESP) was computed at the same B3PW91/6-31G**/LANL2DZ*(Pd) level as above using Gaussian09.[30] The MESP has been shown to be weakly sensitive to the level of calculation.[33] Visualization of the isodensity surfaces color coded with the MESP were performed using Molden.[34] AIM[27] analysis was performed with the TopMoD package.[35] Energy decomposition analyses for optimized structures (PCM-B3PW91/6-31G**/LANL2DZ*(Pd) level) were performed with the ADF 2008.01 program,[36] following the implemented Morokuma−Rauk−Ziegler partition scheme[37] and using the PBEPBE functional in combination with STO-type all-electron basis sets of TZP quality.[38] Scalar relativistic effects were taken into account in all EDA calculations using the ZORA Hamiltonian. Molecular orbitals were plotted using the GABEDIT program.[39]

EXPERIMENTAL SECTION

General Remarks. THF and diethyl ether were dried and distilled over sodium/benzophenone, pentane, dichloromethane, and acetonitrile over P_2O_5. All other reagents were used as commercially available. All reactions were carried out under an argon atmosphere using Schlenk and vacuum-line techniques. The following analytical instruments were used. ^1H, ^{13}C, and ^{31}P NMR: Bruker ARX 250, DPX 300, and Avance 500. NMR chemical shifts δ are in ppm, with positive values to high frequency relative to the tetramethylsilane reference for ^1H and ^{13}C and to the H_3PO_4 reference for ^{31}P; coupling constants J are in Hertz. Diphosphines **1** and **3** were prepared according to a recently reported procedure.[11]

Synthesis of Diphosphine 2. To a solution of **1** (0.62 g, 1.07 mmol) in CH_2Cl_2 (20 mL) cooled at −78 °C was added MeOTf (0.11 mL, 0.96 mmol). The mixture was stirred at room temperature for 2 h. After concentration under vacuum, the residue was washed with Et_2O (40 mL) to afford a white solid (yield 0.56 g, 70%).

^1H NMR (CD_3CN, 25 °C): 7.79 (br s, 1H, H_{ar}), 7.64−7.60 (m, 4H, H_{ar}), 7.57−7.54 (m, 4H, H_{ar}), 7.50−7.45 (m, 3H, H_{ar}), 7.43−7.30 (m, 12H, H_{ar}), 7.25−7.21 (m, 2H, H_{ar}), 7.11 (d, J_{HH} = 9.2 Hz, 1H, H_{ar}), 6.95 (br s, 1H, H_{ar}), 3.22 (s, 3H, CH_3). ^{13}C NMR (CD_3CN, 25 °C): 145.5 (d, J_{CP} = 57.4 Hz, C), 134.1−133.5 (m, 5 CH), 132.3 (d, J_{CP} = 18.9 Hz, CH), 132.2 (CH), 131.8 (CH), 131.4 (CH), 130.9 (m, C), 130.6 (d, J_{CP} = 5.8 Hz, CH), 130.4 (d, J_{CP} = 4.1 Hz, CH), 130.0 (d, J_{CP} = 8.3 Hz, CH), 129.8 (d, J_{CP} = 3.0 Hz, CH), 129.7 (d, J_{CP} = 6.1 Hz, CH), 129.5 (CH), 129.4 (CH), 129.2 (CH), 128.4 (CH), 127.5 (d, J_{CP} = 7.1 Hz, C), 127.3 (d, J_{CP} = 7.2 Hz, C), 121.2 (q, J_{CF} = 322.0 Hz, $CF_3SO_3^-$), 38.1 (CH_3). ^{31}P NMR (CD_3CN, 25 °C): −22.9 (d, J_{PP} = 28.3 Hz), −31.8 (d, J_{PP} = 28.3 Hz). MS (ESI^+): m/z = 593 $[M]^+$. HRMS (ESI^+): calcd for $C_{37}H_{31}N_4P_2$ 593.2024; found 593.1993.

Synthesis of Complex 4. A mixture of complex $PdCl_2(PhCN)_2$ (0.066 g, 0.17 mmol) and **1** (0.10 g, 0.17 mmol) was dissolved in THF (5 mL) at −30 °C and then stirred at room temperature for 3 h. After concentration under vacuum, the residue was washed with Et_2O (5 mL), affording an orange solid (yield 0.12 g, 94%). Recrystallization at room temperature from $CHCl_3$ afforded yellow crystals (mp 245−250 °C).

^1H NMR ($CDCl_3$, 25 °C): 7.86−7.90 (m, 4H, H_{ar}), 7.62−7.65 (m, 2H, H_{ar}), 7.51 (d, J_{HH} = 0.9 Hz, 2H, H_{ar}), 7.32−7.41 (m, 10H, H_{ar}), 7.10−7.14 (m, 2H, H_{ar}), 6.84−6.91 (m, 8H, H_{ar}). ^{13}C NMR ($CDCl_3$, 25 °C): 140.2 (d, J_{CP} = 89.8 Hz, C), 134.3 (d, J_{CP} = 11.3 Hz, CH), 132.9 (d, J_{CP} = 12.2 Hz, CH), 132.1 (d, J_{CP} = 10.4 Hz, CH), 131.8 (CH), 131.3 (d, J_{CP} = 65.4 Hz, C), 131.0 (CH), 130.8 (CH), 130.5 (CH), 130.3 (dd, J_{CP} = 3.8 Hz, J_{CP} = 57.9 Hz, C), 127.8 (d, J_{CP} = 12.8 Hz, CH), 127.8 (d, J_{CP} = 12.1 Hz, CH), 126.6 (CH). ^{31}P NMR ($CDCl_3$, 25 °C): 8.76. MS (ESI^+): m/z = 719 $[M - Cl]^+$. HRMS (ES^+): calcd for $C_{36}H_{28}N_4P_2$-PdCl 719.0522; found 719.0503.

Synthesis of Complex 5. A mixture of complex $PdCl_2(PhCN)_2$ (0.46 g, 1.21 mmol) and **2** (0.90 g, 1.21 mmol) was dissolved in THF (30 mL) at −30 °C and then stirred at room temperature for 3 h. After concentration under vacuum, the residue was washed with Et_2O (40 mL), affording an orange solid (yield 1.01 g, 91%). Recrystallization at room temperature from CH_2Cl_2 afforded orange crystals (mp 188−190 °C).

^1H NMR (CD_3CN, 25 °C): 8.33 (dd, J_{HP} = 13.4 Hz, J_{HH} = 1.2 Hz, 1H, H_{ar}), 8.31 (dd, J_{HP} = 13.3 Hz, J_{HH} = 1.2 Hz, 1H, H_{ar}), 8.26 (t, J_{HP} = J_{HH} = 2.3 Hz, 1H, H_{ar}), 8.01 (d, J_{HH} = 1.8 Hz, 1H, H_{ar}), 7.81−7.88 (m, 2H, H_{ar}), 7.61−7.78 (m, 8H, H_{ar}), 7.41−7.50 (m, 3H, H_{ar}), 7.33−7.38 (m, 4H, H_{ar}), 7.21−7.24 (m, 1H, H_{ar}), 7.10−7.14 (m, 2H, H_{ar}), 6.86 (pseudo td, J_{HH} = 7.6 Hz, J_{HP} = 3.3 Hz, 2H, H_{ar}), 5.75 (br.s, 2H, H_{ar}), 3.05 (s, 3H, CH_3). ^{13}C NMR (CD_3CN, 25 °C): 139.5 (dd, J_{CP} = 4.0 and 88.7 Hz, C), 135.9 (d, J_{CP} = 43.7 Hz, C), 133.3 (d, J_{CP} = 9.7 Hz, CH), 133.2 (d, J_{CP} = 6.6 Hz, CH), 133.1 (d, J_{CP} = 11.6 Hz, CH), 132.9 (d, J_{CP} = 11.1 Hz, CH), 132.8 (d, J_{CP} = 11.2 Hz, CH), 132.4 (CH), 132.3 (CH), 132.1 (d, J_{CP} = 2.9 Hz, CH), 132.0 (d, J_{CP} = 3.5 Hz, CH), 132.0 (C), 131.7 (d, J_{CP} = 3.1 Hz, CH), 131.1 (C), 131.1 (CH), 130.9 (CH), 130.8 (CH), 130.7 (d, J_{CP} = 10.0 Hz, CH), 130.5 (CH), 130.4 (d, J_{CP} = 66.7 Hz, C), 129.5 (d, J_{CP} = 10.6 Hz, CH), 129.4 (d, J_{CP} = 12.6 Hz, CH), 128.9 (d, J_{CP} = 12.9 Hz, CH), 128.2 (dd, J_{CP} = 2.7 and 63.0 Hz, C), 128.2 (d, J_{CP} = 1.8 Hz, CH), 128.0 (d, J_{CP} = 12.5 Hz, CH), 126.2 (d, J_{CP} = 64.2 Hz, C), 122.3 (dd, J_{CP} = 6.0 and 47.0 Hz, C), 121.2 (q, J_{CF} = 320.8 Hz, $CF_3SO_3^-$), 40.2 (CH_3). ^{31}P NMR (CD_3CN, 25 °C): 10.64 (s); 4.10 (s). MS (ESI^+): m/z = 771 $[M]^+$. HRMS (ESI^+) calcd for $C_{37}H_{31}N_4P_2$-(104)$PdCl_2$ 767.0441; found 767.0497.

Synthesis of Complex 6. A mixture of complex $PdCl_2(PhCN)_2$ (0.084 g, 0.22 mmol) and **3** (0.20 g, 0.22 mmol) was dissolved in THF

(10 mL) at −30 °C and then stirred at room temperature for 3 h. After concentration under vacuum, the residue was washed with Et_2O (10 mL), affording an orange solid (yield 0.22 g, 92%). Recrystallization at room temperature from CH_3CN/Et_2O afforded orange crystals (mp 198−200 °C).

^{1}H NMR (CD_3CN, 25 °C): 8.19 (d, J_{HP} = 2.0 Hz, 2H, H_{ar}), 8.08 (br. d, J_{HH} = 5.5 Hz, 4H, H_{ar}), 7.85−7.92 (m, 4H, H_{ar}), 7.80 (t, J_{HH} = 7.5 Hz, 2H, H_{ar}), 7.64−7.73 (m, 12H, H_{ar}), 7.21−7.24 (m, 2H, H_{ar}), 7.14−7.17 (m, 2H, H_{ar}), 3.44 (s, 6H, CH_3). ^{13}C NMR (CD_3CN, 25 °C): 144.5 (t, J_{CP} = 17.8 Hz, C), 138.3 (t, J_{CP} = 8.3 Hz, CH), 135.3 (t, J_{CP} = 6.1 Hz, CH), 135.0 (CH), 133.7 (CH), 133.2 (CH), 132.8 (CH), 130.4 (C), 130.2 (t, J_{CP} = 6.0 Hz, CH), 130.0 (CH), 129.7 (t, J_{CP} = 5.9 Hz, CH), 127.6 (CH), 124.1 (t, J_{CP} = 28.8 Hz, C), 121.3 (q, J_{CF} = 320.9 Hz, $CF_3SO_3^-$), 120.9 (t, J_{CP} = 23.1 Hz, C), 39.5 (CH_3). ^{31}P NMR (CD_3CN, 25 °C): 9.21. MS (ESI$^+$): m/z = 935 [$M^{2+} - CF_3SO_3^-$]$^+$. HRMS (ESI$^+$) calcd for $C_{39}H_{34}N_4P_2PdClF_3SO_3$ 900.0506; found 900.0505.

Crystal Structure Determination of Ligands 1 and 3 and Complexes 4−6. Intensity data were collected at 180 K on Apex2 Bruker or a Xcalibur Oxford Diffraction diffractometer using a graphite-monochromated Mo Kα radiation source and equipped with an Oxford Cryosystems Cryostream Cooler Device. The structures were solved by direct methods and refined by full-matrix least-squares procedures on F using the programs of the PC version of CRYSTALS. Atomic scattering factors were taken from the International Tables for X-ray Crystallography. All non-hydrogen atoms (excepted water molecules for **5**) were refined anisotropically. Hydrogen atoms were located in a difference map (those attached to carbon atoms were repositioned geometrically) and then refined using a riding model. Absorption corrections were introduced using the program MULTISCAN.

Crystal Data of ***1***. $C_{36}H_{28}N_4P_2$, M = 578.59 g·mol^{-1}, monoclinic, a = 49.677(3) Å, b = 8.5858(5) Å, c = 14.3598(9) Å, β = 94.008(3)°, V = 6109.8(6)Å^3, space group $C2/c$, Z = 8, μ(Mo Kα) = 0.174 mm^{-1}, 75 237 reflections measured, 5014 unique (R_{int} =0.055), 379 parameters, 3828 reflections used in the calculations [$I > 0.7\sigma(I)$], R1 = 0.0487, wR2 = 0.0578.

Crystal Data of ***3***. $C_{40}H_{34}F_6N_4O_6P_2S_2$, M = 906.77 g·mol^{-1}, monoclinic, a = 30.774(3) Å, b = 12.2594(14) Å, c = 28.281(3) Å, β = 105.148(4)°, V = 10 299(2) Å^3, space group $C2/c$, Z = 8, μ(Mo Kα) = 0.229 mm^{-1}, 75 266 reflections measured, 8001 unique (R_{int} = 0.079), 544 parameters, refinement on F^2, [$I > 2\sigma(I)$], R1 = 0.0810, wR2 = 0.2048.

Crystal Data of ***4***. $C_{38}H_{30}Cl_8N_4P_2Pd$, M = 994.65 g·mol^{-1}, monoclinic, a = 12.7655(4) Å, b = 16.8290(5) Å, c = 18.7918(6) Å, β = 94.954(3)°, V = 4022.0(2) Å^3, space group $P2_1/n$, Z = 4, μ(Mo Kα) = 1.108 mm^{-1}, 38 029 reflections measured, 10 770 unique (R_{int} = 0.068), 478 parameters, 4855 reflections used in the calculations [$I > 1.9\sigma(I)$], R1 = 0.0298, wR2 = 0.0347.

Crystal Data of ***5***. $C_{38}H_{37}Cl_2F_3N_4O_6P_2PdS$, M = 974.05 g·mol^{-1}, monoclinic, a = 9.3420(4) Å, b = 26.2671(8) Å, c = 17.4220(5) Å, β = 93.916(5)°, V = 4265.1(3) Å^3, space group $P2_1/c$, Z = 4, μ(Mo Kα) = 0.746 mm^{-1}, 46 239 reflections measured, 10 316 unique (R_{int} = 0.081), 511 parameters, 6247 reflections used in the calculations [$I > 3\sigma(I)$], R1 = 0.0518, wR2 = 0.0551.

Crystal Data of ***6***. $C_{44}H_{40}Cl_2F_6N_6O_6P_2PdS_2$, M = 1166.21 g·mol^{-1}, monoclinic, a = 16.8049(4) Å, b = 16.7864(4) Å, c = 17.5998(5) Å, β = 103.697(3)°, V = 4823.6(2) Å^3, space group $P2_1/n$, Z = 4, μ(Mo Kα) = 0.726 mm^{-1}, 45 594 reflections measured, 12 882 unique (R_{int} = 0.060), 622 parameters, 6390 reflections used in the calculations [$I > 1.6\sigma(I)$], R1 = 0.0299, wR2 = 0.0330.

AUTHOR INFORMATION

Corresponding Author

*E-mail: yves.canac@lcc-toulouse.fr (Y.C.); chauvin@lcc-toulouse.fr (R.C.). Fax: (+33)5 61 55 30 03.

ACKNOWLEDGMENT

Beyond the Ministère de l'Enseignement Supérieur de la Recherche et de la Technologie and the Université Paul Sabatier, the authors thank the Centre National de la Recherche Scientifique for the postdoctoral fellowship of N.D. and french public funding for research (ANR-08-JCJC-0137-01). Theoretical studies were performed using HPC resources from CALMIP (Grant 2009 and 2010 [0851]]) and from GENCI-[CINES/IDRIS] (Grant 2009 and 2010 [085008]).

ASSOCIATED CONTENT

Supporting Information. Calculation details. This material is available free of charge via the Internet at http://pubs.acs.org.

REFERENCES

(1) (a) James, S. L. *Chem. Soc. Rev.* **2009**, *38*, 1744. (b) Freixa, Z.; van Leeuwen, P. W. N. M. *Coord. Chem. Rev.* **2008**, *252*, 1755.

(2) (a) van Leeuwen, P. W. N. M.; Kamer, P. C. J.; Reek, J. N. H.; Dierkes, P. *Chem. Rev.* **2000**, *100*, 2741. (b) Kamer, P. C. J.; van Leeuwen, P. W. N. M.; Reek, J. N. H. *Acc. Chem. Res.* **2001**, *34*, 895. (c) Ding, K.; Miller, D. L.; Young, V. G.; Lu, C. C. *Inorg. Chem.* **2011**, *50*, 2545.

(3) Destefano, N. J.; Johnson, D. K.; Lane, R. M.; Venanzi, L. M. *Helv. Chim. Acta* **1976**, *59*, 2674.

(4) Devon, T. J.; Phillips, G. W.; Puckette, T. A.; Stravinoha, J. L.; Vanderbilt, J. J. U.S. Patent, 4,694,109, Sept 15, 1986.

(5) Sawamura, M.; Hamashima, H.; Ito, Y. *Tetrahedron: Asymmetry* **1991**, *2*, 593.

(6) (a) Schuecker, R.; Mereiter, K.; Spindler, F.; Weissensteiner, W. *Adv. Synth. Catal.* **2010**, *352*, 1063. (b) Birkholz, M. N.; Freixa, Z.; van Leeuwen, P. W. N. M. *Chem. Soc. Rev.* **2009**, *38*, 1099.

(7) Aguilà, D.; Escribano, E.; Speed, S.; Talancón, D.; Yermán, L.; Alvarez, S. *Dalton Trans.* **2009**, 6610.

(8) (a) Freiza, Z.; Beentjes, M. S.; Batema, G. D.; Dieleman, C. B.; van Strijdonck, G. P. F.; Reek, J. N. H.; Kamer, P. C. J.; Fraanje, J.; Goubitz, K.; van Leeuwen, P. W. N. M. *Angew. Chem., Int. Ed.* **2003**, *42*, 1284.

(9) (a) Poorters, L.; Armspach, D.; Matt, D.; Toupet, L.; Choua, S.; Turek, P. *Chem.—Eur. J.* **2007**, *13*, 9448. (b) Poorters, L.; Lejeune, M.; Armspach, D.; Matt, D. *Actual. Chim.* **2009**, *326*, 15.

(10) SPANphos is a trans-spanning diphosphine that has also been reported to act as a cis-chelating ligand. See: Jiménez-Rodríguez, C.; Roca, F. X.; Bo, C.; Benet-Buchholz, J.; Escudero-Adán, E. C.; Freixa, Z.; van Leeuwen, P. W. N. M. *Dalton Trans.* **2006**, 268.

(11) Canac, Y.; Debono, N.; Vendier, L.; Chauvin, R. *Inorg. Chem.* **2009**, *48*, 5562.

(12) See for examples:(a) Brunet, J.-J.; Chauvin, R.; Commenges, G.; Donnadieu, B.; Leglaye, P. *Organometallics* **1996**, *15*, 1752. (b) Brunet, J. J.; Chauvin, R.; Chiffre, J.; Huguet, S.; Leglaye, P. *J. Organomet. Chem.* **1998**, *566*, 117. (c) Chauvin, R. *Eur. J. Inorg. Chem.* **2000**, 577. (d) Zurawinski, R.; Lepetit, C.; Canac, Y.; Vendier, L.; Mikolajczyk, M.; Chauvin, R. *Tetrahedron: Asymmetry* **2010**, *21*, 1777.

(13) (a) Wilkinson, M. J.; Van Leeuwen, P. W. N. M.; Reek, J. N. H. *Org. Biomol. Chem.* **2005**, *3*, 2371. (b) Breit, B. *Angew. Chem., Int. Ed.* **2005**, *44*, 6816. (c) Gulyás, H.; Benet-Buchholz, J.; Escudero-Adan, E. C.; Freixa, Z.; Van Leeuwen, P. W. N. M. *Chem.—Eur. J.* **2007**, *13*, 3424.

(14) (a) Snelders, D. J. M.; Siegler, M. A.; von Chrzanowski, L. S.; Spek, A. L.; van Koten, G.; Klein Gebbink, R. J. M. *Dalton Trans* **2011**, 2588. (b) Snelders, D. J. M.; van Koten, G.; Klein Gebbink, R. J. M. *Chem.—Eur. J.* **2011**, *17*, 42. (c) Harper, B. A.; Knight, D. A.; George, C.; Brandow, S. L.; Dressick, W. J.; Dalcey, C. S.; Schull, T. L. *Inorg. Chem.* **2003**, *42*, 516. (d) Hessler, A.; Kucken, S.; Stelzer, O.; Blotevogel-Baltronat, J.; Sheldrick, W. S. *J. Organomet. Chem.* **1995**, *501*, 293.

(e) Francisco, L. W.; Moreno, D. A.; Atwood, J. D. *Organometallics* **2001**, *20*, 4237.

(15) (a) Pearson, R. G. *Inorg. Chem.* **1973**, *12*, 712. (b) Navarro, R.; Urriolabeitia, E. P. *J. Chem. Soc., Dalton Trans.* **1999**, 4111. (c) Harvey, J. N.; Heslop, K. M.; Orpen, A. G.; Pringle, P. G. *Chem. Commun.* **2003**, 278.

(16) (a) Abdellah, I.; Lepetit, C.; Canac, Y.; Duhayon, C.; Chauvin, R. *Chem.—Eur. J.* **2010**, *16*, 13095. (b) Abdellah, I.; Boggio-Pasqua, M.; Canac, Y.; Lepetit, C.; Duhayon, C.; Chauvin, R. *Chem.—Eur. J.* **2011**, *17*, 5110.

(17) CCDC-829643 (**1**), CCDC-829642 (**3**), CCDC-829640 (**4**), CCDC-829644 (**5**), and CCDC-829641 (**6**) contain supplementary crystallographic data for this paper. This data can be obtained free of charge from the Cambridge Crystallographic Data Centre via www.ccdc.cam.ac.uk/data_request/cif.

(18) Noteworthy, probably due to a decrease of nucleophilic character, attempted methylation of the sp^2 nitrogen atom of the imidazole ring after coordination to palladium failed.

(19) (a) Debono, N.; Canac, Y.; Duhayon, C.; Chauvin, R. *Eur. J. Inorg. Chem.* **2008**, 2991. (b) Abdellah, I.; Debono, N.; Canac, Y.; Vendier, L.; Chauvin, R. *Chem. Asian J.* **2010**, *5*, 1225.

(20) (a) Zhao, Y. X.; Wang, S. G. *Chin. Chem. Lett.* **2005**, *16*, 1555. (b) Zurawinski, R.; Lepetit, C.; Canac, Y.; Mikolajczyk, M.; Chauvin, R. *Inorg. Chem.* **2009**, *48*, 2147.

(21) In the rhodium(I) series, the dicationic ligand **3** of **6** may behave in either a cis- or a trans-chelating manner. In the crystal state, however, the corresponding shortest distance between N-methyl and P-phenyl substituents was even found to be shorter in the trans isomer (ca. 3.09 Å) than in the cis isomer (ca. 3.16 Å).[11]

(22) County, A. *Comprehensive Organometallic Chemistry III*; Elsevier: Oxford, 2007; Vol. 8.

(23) (a) Morokuma, K. *J. Chem. Phys.* **1971**, *55*, 1236. (b) Kitaura, K.; Morokuma, K. *Int. J. Quantum Chem.* **1976**, *10*, 325. (c) Ziegler, T.; Rauk, A. *Theor. Chim. Acta* **1977**, *46*, 1.

(24) In principle, application of the EDA method for investigation of the role of electrostatics in determination of the cis/trans stereochemical preference of ligands **1**−**3** is also a priori envisageable. It would require an unusual fragmentation of the ligands for separating the two imidazolylphosphine moieties where positive charges are possibly located. Such a fragmentation, e.g., as $ImPh_2(C_3H_2)PPdCl_2 + Im'Ph_2(C_3H_2)P$ (where Im and Im′ stand for neutral or methylated imidazolyl substituents), is however unatural and would require difficult treatment of open-shell (carbene-radical) species.

(25) Antonova, N. S.; Carbÿo, J. J.; Poblet, J. M. *Organometallics* **2009**, *28*, 4283.

(26) Jacobsen, H.; Correa, A.; Poater, A.; Costabile, C.; Cavallo, L. *Coord. Chem. Rev.* **2009**, *253*, 687.

(27) Bader, R. F. W. *Atoms in Molecules*; Clarendon Press: Oxford, 1990.

(28) (a) Sorocco, E.; Tomasi, J. *Adv. Quantum Chem.* **1978**, *11*, 116. (b) Sorocco, E.; Tomasi, J. In *Chemical Applications of Atomic and Molecular Electrostatic potentials*; Politzer, P., Thruhlar, D. G., Eds.; Plenum: New York, 1981. (c) Politzer, P.; Murray, J. S. *Theor. Chem. Acc.* **2002**, *108*, 134.

(29) (a) Gadre, S. R.; Kulkarni, S. A.; Shrivastava, I. H. *J. Chem. Phys.* **1992**, *96*, 5253.(b) Gadre, S. R. In *Comprehensive Chemistry, Reviews in Current Trends*; Leczynski, J., Ed.; World Scientific: Singapore, 2000; Vol. 4, p 1. (c) Gadre, S. R.; Shirsat, R. N. *Electrostatics of Atoms and Molecules*; Universities Press: Hyderabad, India, 2000.

(30) Frisch, M. J.; Trucks, G. W.; Schlegel, H. B.; Scuseria, G. E.; Robb, M. A.; Cheeseman, J. R.; Scalmani, G.; Barone, V.; Mennucci, B.; Petersson, G. A.; Nakatsuji, H.; Caricato, M.; Li, X.; Hratchian, H. P.; Izmaylov, A. F.; Bloino, J.; Zheng, G.; Sonnenberg, J. L.; Hada, M.; Ehara, M.; Toyota, K.; Fukuda, R.; Hasegawa, J.; Ishida, M.; Nakajima, T.; Honda, Y.; Kitao, O.; Nakai, H.; Vreven, T.; Montgomery, Jr., J. A.; Peralta, J. E.; Ogliaro, F.; Bearpark, M.; Heyd, J. J.; Brothers, E.; Kudin, K. N.; Staroverov, V. N.; Kobayashi, R.; Normand, J.; Raghavachari, K.; Rendell, A.; Burant, J. C.; Iyengar, S. S.; Tomasi, J.; Cossi, M.; Rega, N.; Millam, N. J.; Klene, M.; Knox, J. E.; Cross, J. B.; Bakken, V.; Adamo, C.; Jaramillo, J.; Gomperts, R.; Stratmann, R. E.; Yazyev, O.; Austin, A. J.; Cammi, R.; Pomelli, C.; Ochterski, J. W.; Martin, R. L.; Morokuma, K.; Zakrzewski, V. G.; Voth, G. A.; Salvador, P.; Dannenberg, J. J.; Dapprich, S.; Daniels, A. D.; Farkas, Ö.; Foresman, J. B.; Ortiz, J. V.; Cioslowski, J.; Fox, D. J. *Gaussian 09*, Revision A.1; Gaussian, Inc.: Wallingford, CT, 2009.

(31) Ehlers, A. W.; Böhme, M.; Dapprich, S.; Gobbi, A.; Höllwarth, A.; Jonas, V.; Köhler, K. F.; Stegmann, R.; Veldkamp, A.; Frenking, G. *Chem. Phys. Lett.* **1993**, *208*, 111.

(32) Pye, C. C.; Ziegler, T. *Theor. Chem. Acc.* **1999**, *101*, 396.

(33) Kulkarni, S. A.; Gadre, S. R. *Chem. Phys. Lett.* **1997**, *274*, 255.

(34) Schaftenaar, G. *Molden software*; CMBI: http://www.cmbi.ru.nl/molden/molden.html.

(35) Noury, S.; Krokidis, X.; Fuster, F.; Silvi, B. *Comput. Chem.* **1999**, *23*, 597.

(36) (a) te Velde, G.; Bickelhaupt, F. M.; van Gisbergen, S. J. A.; Fonseca Guerra, C.; Baerends, E. J.; Snijders, J. G.; Ziegler, T. Chemistry with ADF *J. Comp. Chem.* **2001**, *22*, 931. (b) Snijders, G.; te Velde Baerends, E. J. *Towards an order-N DFT method*. Theoretical Chemistry Accounts **99**, 391 (1998) (c) ADF2008.01; SCM, Theoretical Chemistry, Vrije Universiteit: Amsterdam, The Netherlands, http://www.scm.com

(37) (a) Ziegler, T.; Rauk, A. *Inorg. Chem.* **1979**, *18*, 1558. (b) Ziegler, T.; Rauk, A. *Inorg. Chem.* **1979**, *18*, 1755. (c) Bickelhaupt, F. M.; Baerends, E. J. In *Reviews in Computational Chemistry*; Lipkowitz, K. B., Boyd, D. B., Eds.; Wiley: New York, 2000; Vol. 15, pp 1−86.

(38) Van Lenthe, E.; Baerends, E. J. *J. Comput. Chem.* **2003**, *24*, 1142.

(39) http://sites.google.com/site/allouchear/Home/gabedit.